LCC-0068
June 2001

Linear Collider Collaboration Tech Notes

Radial Particle Distribution on Two DDS2 Cells

F. Marcelja and E. L. Garwin

Stanford Linear Accelerator Center
Stanford, CA

Abstract: Search for particles, as the cause of breakdown, was performed on DDS2 cells 86 and 20.

Radial Particle Distribution on Two DDS2 cells

F. Marcelja and E. Garwin, Stanford Linear Accelerator Center
Stanford University, Stanford, CA 94309

±*Abstract: Search for particles, as the causes of breakdown, was performed on DDS2 cells 86 and 20.*

1 Introduction

We present some further examination of DDS2 cells #86 and #20, previously described in ref.1. While there the question was about copper loss causing a tune shift, here we are interested in correlation of breakdown with possible precursors. Particle contamination, if present, at the time of RF application could be such a precursor. We searched for particles on the irises of both cells. The particles could have landed there, or have been removed, at any time during the experiment.

2 Experimental Details

The search area for both cells was a rectangular strip oriented in radial direction. We did not limit the search to breakdown areas; in fact we tried to exclude them by discarding the particle search candidate if its X-ray intensity due to Cu was > 95% of total. Even with the reject condition active we collected many events of Cu breakdown type and these were rejected manually from the final list.

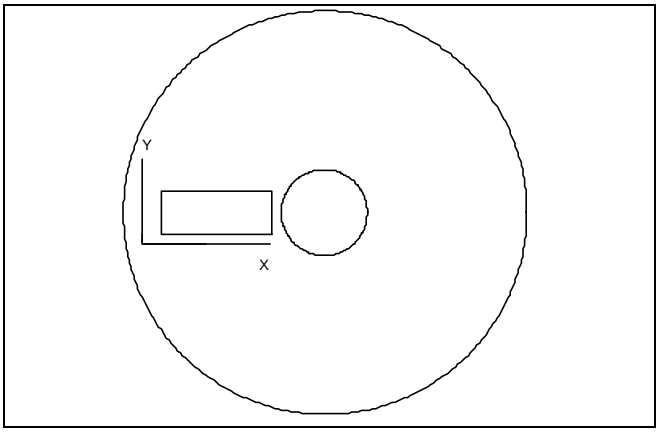

Fig.1. Sketch showing the rectangular search area in Fig. 2 and Fig. 4

†Work supported by the U.S. Department of Energy under contract number DE-AC03-76SF00515.

We start from automatically collected raw data reported in Table 1 and Table 2 and summarized in the table below

Cell #	Raw # of particles	# / cm square	x-y scatterpl.	Radial distrib.
86	265	6077	Fig.2	Fig.3
20	336	6975	Fig.4	Fig.5

3. Results

Cell #20 is positioned upstream and has more breakdowns than cell #86 which is positioned more downstream in the accelerator structure. Both cells were searched on the beam upstream sides.

As the cell #20 has many breakdown sites, the search for particles was disturbed by false hits. Out of 336 candidates, after careful examination of pictures and spectra, we accepted about 113 particles.

In cell #86 we found 138 particles containing manganese, while in cell #20 we found only 7 such particles. Apart from these the rest of particles was the usual mix. We did not attempt to do any correlation between the particles and the breakdown sites.

The results are reported in form of scatter-plot (Fig.1 and Fig.3), radial distributions (Fig.2 and Fig.4) and statistics compiled by the analysis program (Table 1 and Table 2). At the end we add a few particle pictures with the collected X-ray spectra (Fig.6 and Fig.7).

4. Conclusions

Not much could be concluded from these data as far as the possible statistical correlation of particle sites with breakdowns. On the other hand the manganese contamination should be of some interest and calls for an explanation. MnS was observed on at least one occasion in the past, on a Windowtron test nose. That source was speculated to be the Rf braze furnace but a subsequent braze with another nose showed no MnS contamination. MnS is a common contaminant in Cu-Ni, used in Klystron production.

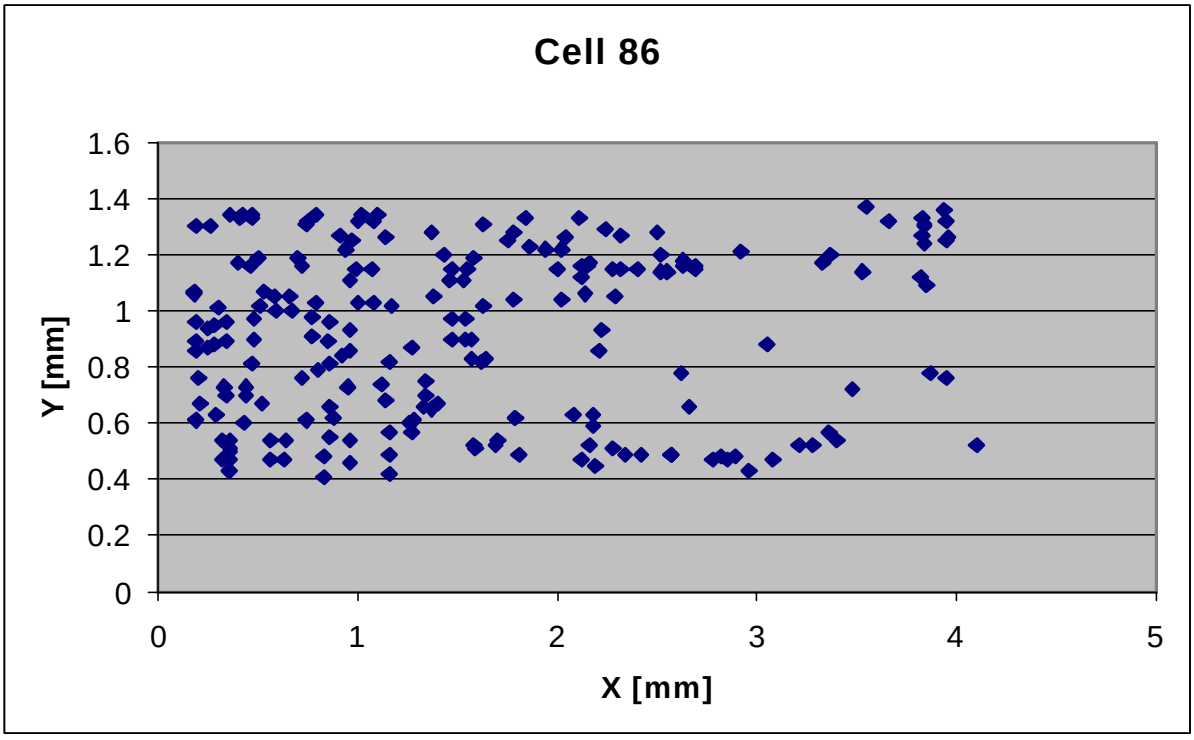

Fig. 2. Positions of particles found in search area as sketched in Fig.1. Cell iris edge is on the right, at X≅4.5 mm

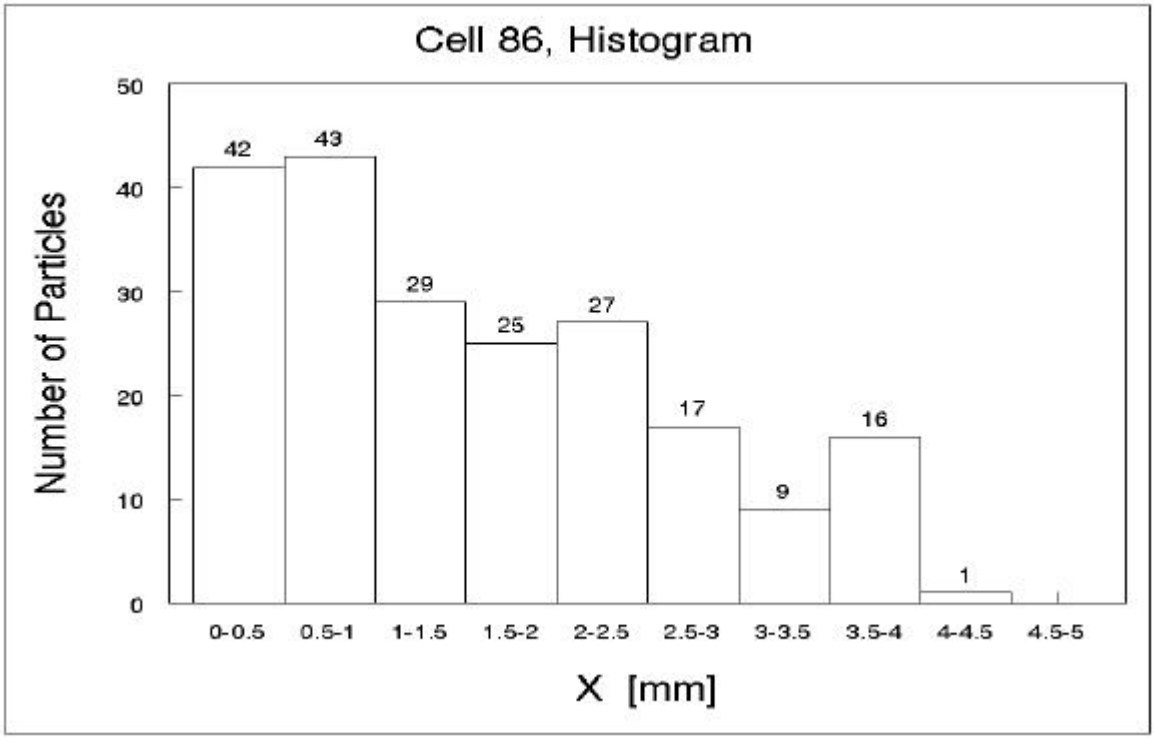

Fig. 3. Histogram data of Fig. 2, projected along X-axis.

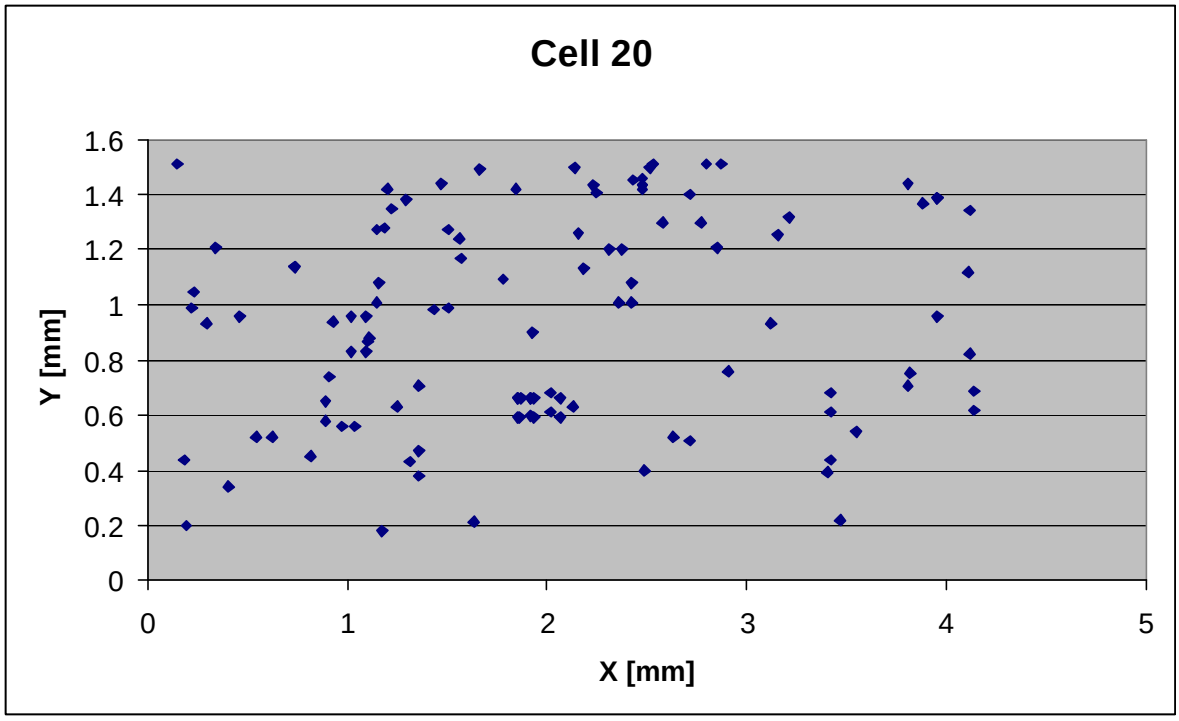

Fig. 4. . Positions of particles found in search area as sketched in Fig.1. Cell iris edge is on the right, at X≅4.5 mm.

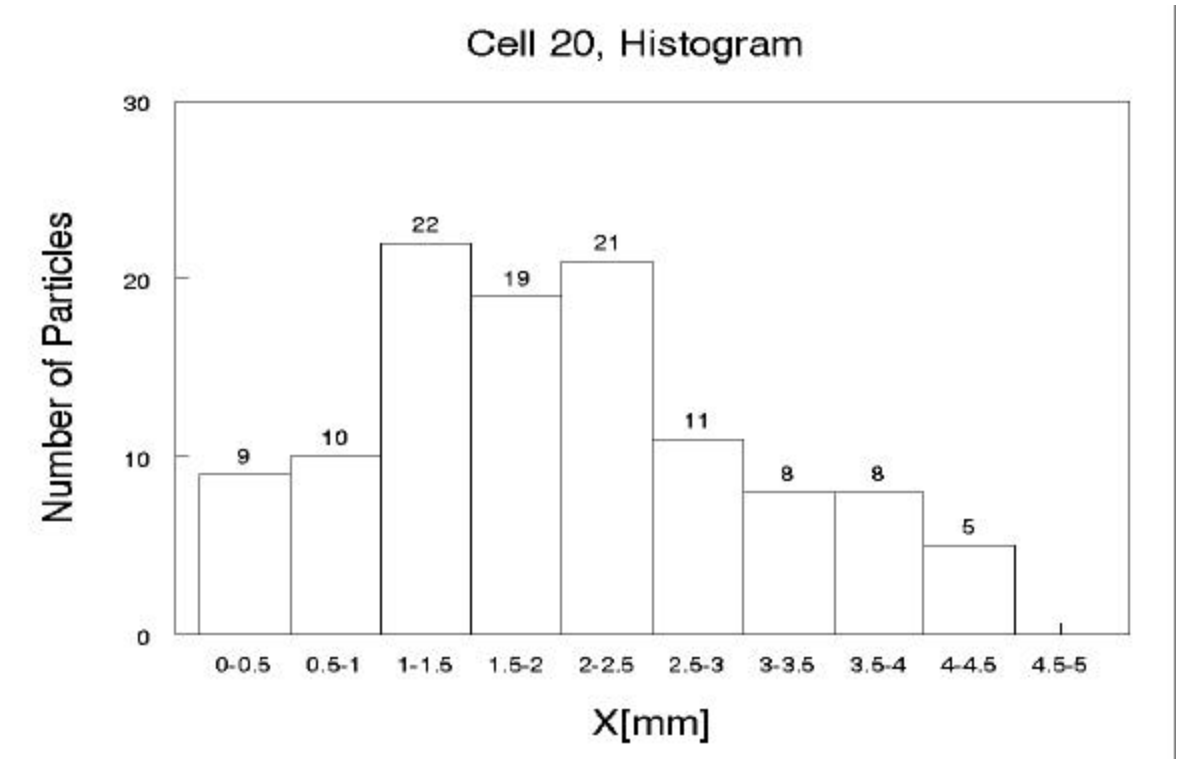

Fig. 5. Histogram data of Fig. 4, projected on X-axis.

Table 1

DataFiles 000071_A\000071_A.*
Sample_Number 86b
Client_Name iris
Analysis_Date 2/20/1
Operator FM

Mag	Fields	Grid
2000	2208.9719	0.174

Classes	#	Number %	Area %	Vol %	Wt %	Counts	Area Fr.	Num/cm^2
S-Mn-Cu	67	25.26	16.12	4.98	5.76	8205	0.0000270	1.535E+003
Cu-Fe- O	50	18.85	8.98	2.73	4.40	4387	0.0000150	1.146E+003
Fe- O- F	22	8.29	16.58	11.23	14.23	6358	0.0000278	5.041E+002
S-Cu-Mn	22	8.29	4.22	1.01	1.29	6581	0.0000071	5.041E+002
Cu- S-Mn	34	12.91	2.96	0.52	0.79	4925	0.0000050	7.845E+002
S-Mn	13	4.90	6.58	2.94	2.90	10168	0.0000110	2.979E+002
Cu- O	17	6.41	4.11	1.27	1.88	3864	0.0000069	3.895E+002
Cu- C	16	6.03	3.61	1.32	2.17	3695	0.0000061	3.666E+002
Al- O	1	0.38	18.98	50.73	50.65	7638	0.0000318	2.291E+001
Fe-Cu- O	5	1.89	2.49	0.82	1.23	5284	0.0000042	1.146E+002
C	1	0.38	8.53	18.50	10.88	9353	0.0000143	2.291E+001
Si-Al- O	2	0.75	3.42	2.36	2.04	14873	0.0000057	4.582E+001
Cu-Si- O	7	2.64	0.84	0.19	0.24	6055	0.0000014	1.604E+002
O-Al	1	0.38	0.89	0.62	0.52	8084	0.0000015	2.291E+001
Fe- F	1	0.38	0.81	0.46	0.66	6219	0.0000014	2.291E+001
Si-Cu-Al	2	0.75	0.31	0.09	0.11	7879	0.0000005	4.582E+001
Ca-Cu- O	1	0.38	0.37	0.17	0.20	5445	0.0000006	2.291E+001
O-Fe-Cu	1	0.38	0.14	0.03	0.05	5110	0.0000002	2.291E+001
Cu-Mn-Ca	1	0.38	0.04	0.00	0.01	3890	0.0000001	2.291E+001
Cu-Pb-Mn	1	0.38	0.03	0.00	0.00	5156	0.0000000	2.291E+001
Totals	265	100.00	100.00	100.00	100.00	6201	0.0001676	6.077E+003

Size Distribution by Average Diameter (microns)

Classes	Number	<1	1.0 to 2.5	2.5 to 5.0	5.0 to 10.0	10.0 to 20.0	20.0 to 50.0	50.0 to 100.0	>100
S-Mn-Cu	67	0	67	0	0	0	0	0	0
Cu-Fe- O	50	16	33	1	0	0	0	0	0
Fe- O- F	22	0	15	6	1	0	0	0	0
S-Cu-Mn	22	2	20	0	0	0	0	0	0
Cu- S-Mn	34	25	9	0	0	0	0	0	0
S-Mn	13	0	11	2	0	0	0	0	0
Cu- O	17	7	9	1	0	0	0	0	0
Cu- C	16	7	8	1	0	0	0	0	0
Al- O	1	0	0	0	0	1	0	0	0
Fe-Cu- O	5	0	4	1	0	0	0	0	0
C	1	0	0	0	1	0	0	0	0
Si-Al- O	2	0	0	2	0	0	0	0	0
Cu-Si- O	7	3	4	0	0	0	0	0	0
O-Al	1	0	0	1	0	0	0	0	0
Fe- F	1	0	0	1	0	0	0	0	0
Si-Cu-Al	2	0	2	0	0	0	0	0	0
Ca-Cu- O	1	0	1	0	0	0	0	0	0
O-Fe-Cu	1	0	1	0	0	0	0	0	0
Cu-Mn-Ca	1	1	0	0	0	0	0	0	0
Cu-Pb-Mn	1	1	0	0	0	0	0	0	0
Totals	265	62	184	16	2	1	0	0	0

Table 2

DataFiles 000072_A\000072_A.*
Sample_Number 20-a
Client_Name iris
Analysis_Date 2/26/1
Operator FM

Mag	Fields	Grid
2000	2593.1516	0.174

Classes	#	Number %	Area %	Vol %	Wt %	Counts	Area Fr.	Num/cm^2
Cu- O 16.3	227	68.89	21.87	5.11	5.86	6030	0.0001379	4.806E+003
Cu- O- C 21.4	9	2.52	18.95	30.20	31.67	5967	0.0001194	1.757E+002
Cu-Cl- O- C 45.5	2	0.56	14.51	24.99	22.57	6799	0.0000915	3.904E+001
Cu- C- O 24.6	5	1.40	13.07	17.35	17.88	6508	0.0000824	9.759E+001
Cu-Si 13.6	14	3.92	8.72	5.80	5.42	9104	0.0000550	2.732E+002
Cu- O-Ca 39.3	6	1.68	5.49	8.17	8.26	7051	0.0000346	1.171E+002
Cu-Ca- O 63.3	14	3.92	3.66	1.51	1.44	7869	0.0000231	2.732E+002
Cu- O-Si 75.0	16	4.48	3.05	0.92	0.93	7415	0.0000192	3.123E+002
Cu-Fe 56.3	5	1.58	3.05	1.59	1.90	6927	0.0000192	1.105E+002
Cu- O-Al 33.3	9	2.52	2.98	2.21	2.31	7404	0.0000188	1.757E+002
Cu- C 19.0	6	1.68	1.04	0.52	0.60	5771	0.0000066	1.171E+002
Si- O- C-Al 75.0	1	0.28	1.04	0.86	0.53	3508	0.0000065	1.952E+001
Si-Cu-Al- O 85.3	2	0.56	0.69	0.32	0.25	13842	0.0000043	3.904E+001
S-Cu-Mn 84.1	7	1.96	0.41	0.07	0.06	10507	0.0000026	1.366E+002
O-Al 75.4	1	0.28	0.36	0.16	0.09	2913	0.0000023	1.952E+001
Cu- S- O 27.5	7	2.38	0.33	0.07	0.07	8120	0.0000021	1.661E+002
Ca-Cu- O-Al 96.4	1	0.28	0.25	0.07	0.06	8356	0.0000016	1.952E+001
Fe- F 35.1	1	0.28	0.24	0.00	0.00	13078	0.0000015	1.952E+001
Fe-Cu-Cr- O 87.2	2	0.56	0.23	0.06	0.07	9351	0.0000014	3.904E+001
Cu-Al- O-Ca 36.0	1	0.28	0.05	0.01	0.01	7902	0.0000003	1.952E+001
Totals	336	100.00	100.00	100.00	100.00	6594	0.0006304	6.975E+003

Size Distribution by Average Diameter (microns)

Classes	Number	<1	1.0 to 2.5	2.5 to 5.0	5.0 to 10.0	10.0 to 20.0	20.0 to 50.0	50.0 to 100.0	>100
Cu- O 16.3	246	120	89	34	3	0	0	0	0
Cu- O- C 21.4	9	0	2	3	2	1	1	0	0
Cu-Cl- O- C 45.5	2	0	0	0	1	0	1	0	0
Cu- C- O 24.6	5	1	0	2	0	2	0	0	0
Cu-Si 13.6	14	0	3	7	3	1	0	0	0
Cu- O-Ca 39.3	6	0	3	2	0	1	0	0	0
Cu-Ca- O 63.3	14	0	4	10	0	0	0	0	0
Cu- O-Si 75.0	16	1	9	5	1	0	0	0	0
Cu-Fe 56.3	6	2	0	2	2	0	0	0	0
Cu- O-Al 33.3	9	1	5	1	2	0	0	0	0
Cu- C 19.0	6	1	4	0	1	0	0	0	0
Si- O- C-Al 75.0	1	0	0	0	1	0	0	0	0
Si-Cu-Al- O 85.3	2	0	0	2	0	0	0	0	0
S-Cu-Mn 84.1	7	0	7	0	0	0	0	0	0
O-Al 75.4	1	0	0	1	0	0	0	0	0
Cu- S- O 27.5	9	5	4	0	0	0	0	0	0
Ca-Cu- O-Al 96.4	1	0	0	1	0	0	0	0	0
Fe- F 35.1	1	0	0	1	0	0	0	0	0
Fe-Cu-Cr- O 87.2	2	1	0	1	0	0	0	0	0
Cu-Al- O-Ca 36.0	1	0	1	0	0	0	0	0	0
Totals	357	131	131	72	16	5	2	0	0

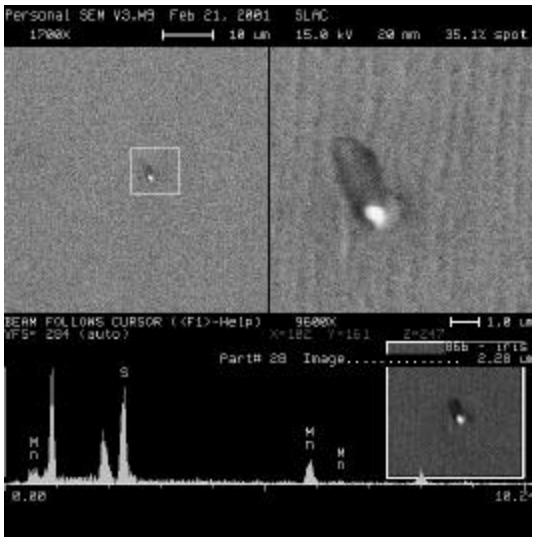

Fig. 6. Particle picture as relocated, enlarged view, X-ray spectrum showing sulfur and manganese, and picture of particle taken automatically during the search.

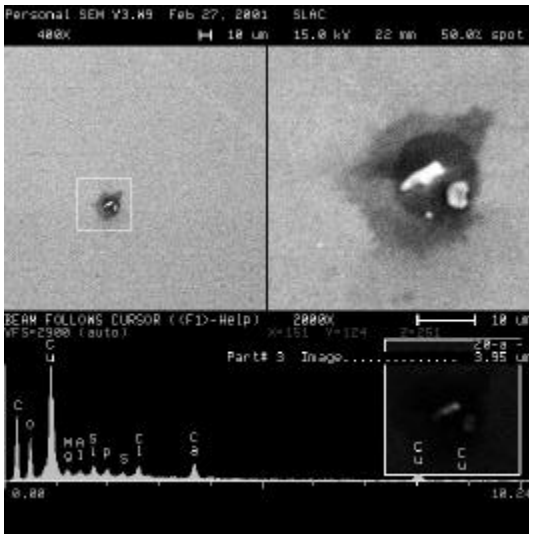

Fig. 7. Another example. Apart from Cu we often find Si, Al, Mg, O together with Ca, and in addition Cl and C.

5. Reference

1. R.E.Kirby and F.Marcelja, DDS2 Structure Autopsy, NLCTA Note 66 (2001)

6. Appendix

Scanning Electron Microscopy (SEM)

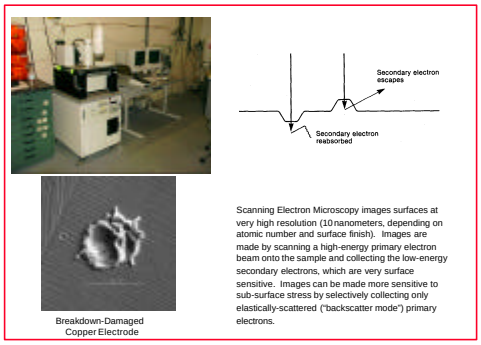

Energy-Dispersive X-Ray Analysis (EDX)

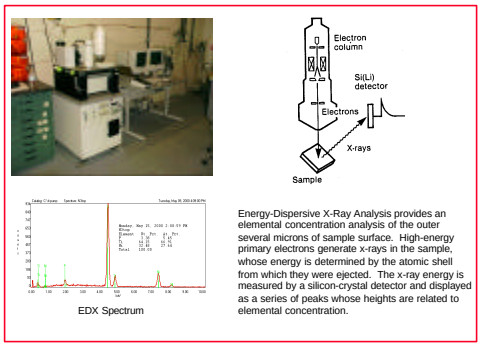

Particle search details: SEM microscope depicted above is equipped with a translation stage controlled by computer. It also has software for automatic search for particles. The search is based on image contrast. Back-scattered electrons are used. Search parameters, like detection threshold, are chosen for a given sample conditions. The energy dispersive X-ray spectra and images of particles are taken during the search. Further acceptance criteria may be based on geometry and X-ray data. Statistical analysis is also provided. Particles can be relocated for further checking.